Ionospheric Tomography by Neural Network Collocation Method

ITC16

December 5-8, 2006

Tatsuoki TAKEDA(UEC)

XiaoFeng MA(Xilisoft Co.)

Contents

1. Introduction

CT by NNCM

*NN is Function expansion with variable basis function

*NNCM is effective for CT with small amount of projection data

Purpose of the CIT research

TEC (Total Electron Contents)

derived from Phase Delay of GPS signals

⇩ Neural network collocation method

Ionospheric electron density distribution

1.1 Ionospheric tomography(CIT)

Purposes of ionospheric tomography

(1) Practical

Aircraft positioning (vertical resolution)

Car navigation (horizontal resolution)

Electro-communications

(2) Academic

Solar-activity

Geo-science

Status of ionospheric tomography

(1) Two-dimensional CIT

a) 1988 Austen, et al.

Model ionosphere ⇨ Model TEC data

Model satellite at 1000 km altitude

3~5 model ground station

ART(algebraic reconstruction technique)

b) 1990 Raymund, et al.

1992 Fremouw, et al.

1995 Kunitake, et al.

Real observation: NNSS 1100 km , polar orb.

(National Navigation Satellite System)

#Limitations

*Dimensionality: Only 2-dim plane formed

by sat. orbit and receivers array

*Observation time and observation place

(2) Vertical profile measurement

a) 1998 Hajj and Romans

2000 Tsai, et al.

Abel inversion by using GPS & LEO satellites

Spherical symmetry is assumed

b) 2003 Garcia-Fernandez, et al.

Vert.-Hor. separable model

Abel inversion by GPS+LEO (vertical)

IRI model (horizontal)

c) 2003 Garcia-Fernandez, et al.

GPS, ionosonde, NeQuick model

*NeQuick model

Input: Position, Time, Solar flux

Output: Electron density at the position

(3) Three dimensional CIT

a) 1997 Hansen, et al.

GPS

Radon transformation

Function expansion

Basis functions derived from IRI model

Practical purpose for ionospheric correction

b) 1998 Hernandes-Pajares, et al.

3D reconstruction

GPS, LEO, ground receivers

Resolution: 10 x 10 deg, 100 km

distance(GPS-LEO) is very long as 1000 km

c) 2005 Ma, et al., (described here)

3D reconstruction, NNCM

GPS, ionosonde

Resolution: 0.5 x 0.5 deg, 30 km

Basic concept of tomographic reconstruction

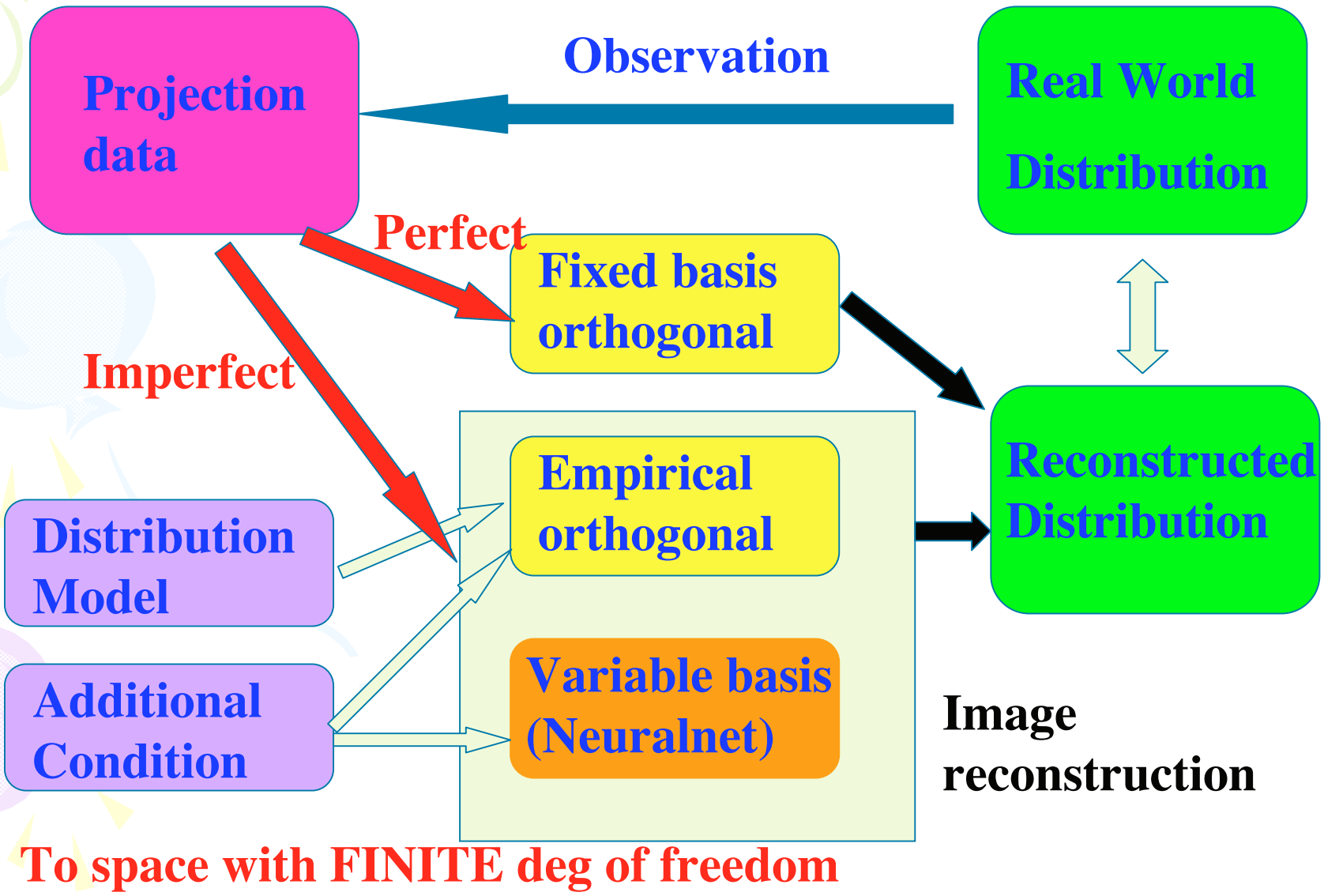

1.2 Neural network basics

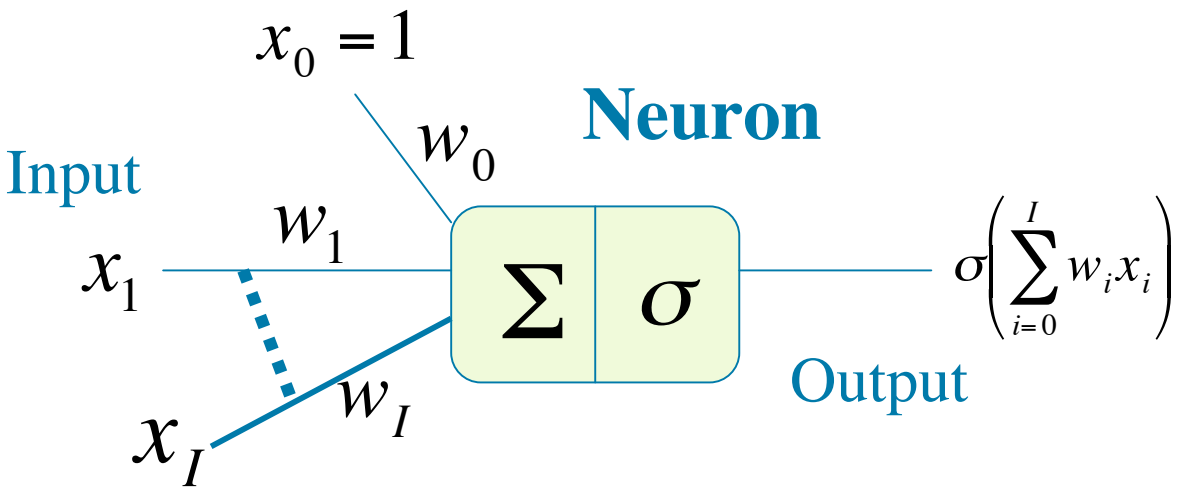

Activation function

$$\sigma(x) = \sigma_1(x) = \frac{1}{1+e^{-x}} \quad \text{Hidden layer}$$

$$\hat{\sigma}(x) = x \quad \text{Output layer(usual)}$$

$$\hat{\sigma}(x) = \sigma_2(x) \quad \text{Output layer}$$

$$= x + \log(1+e^{-x}) \quad \text{(CIT by NNCM)}$$

$$\hat{\sigma}(x) = \sigma_2(x) \qquad \frac{d\hat{\sigma}(x)}{dx} = \sigma_1(x)$$

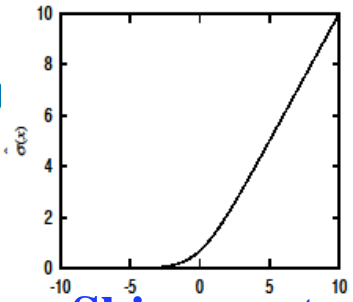

Skimmer-type

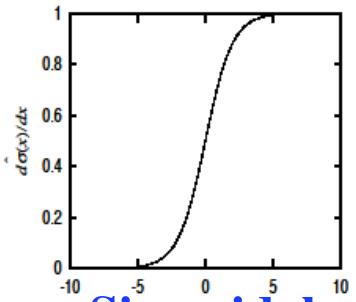

Sigmoidal

(Example) Three layer neural network

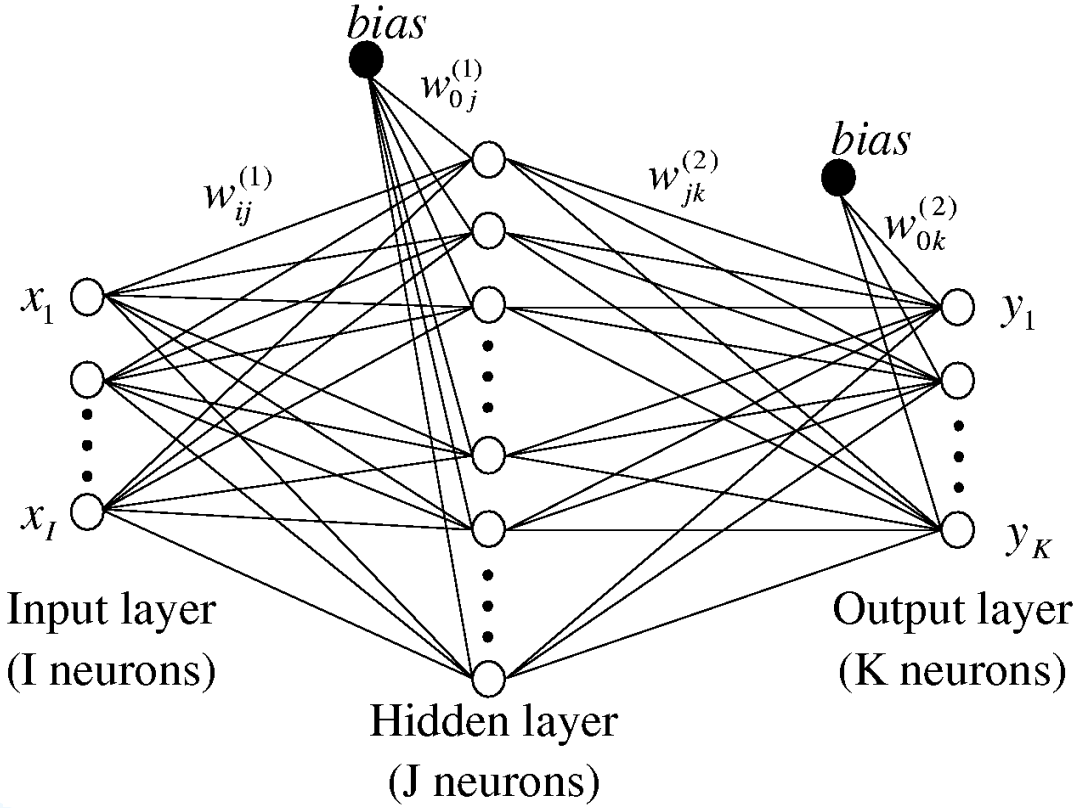

$$y_k = \hat{\sigma}\left\{\sum_{j=1}^{J} w_{jk}^{(2)}\sigma\left(\sum_{i=0}^{I} w_{ij}^{(1)}x_i\right) + w_{0k}^{(2)}\right\}$$

$x_0 = 1, \quad k = 1,\ldots K, \quad \sigma(\cdot), \hat{\sigma}(\cdot)$: Activation functions

Advantageous features of NN for our purpose

(1) It can approximate any functions within any precision under a certain mathematical condition.

(2) Generalization property is controlled by selecting the network structure and iteration number appropriately.

(3) The method is robust against noises in input data.

(4) Wide range of complex nonlinear problems can be solved by selecting the object function appropriately.

A multilayer neural network is considered to be a function expressed by a SERIES of VARIABLE BASIS FUNCTIONS

Conventional function expansion

$$y = f(\vec{x}) \cong g(\vec{x}) \equiv \sum_{n=1}^{N} a_n \phi_n(\vec{x})$$

$\phi_n(\vec{x})$ Fixed basis function

a_n Weight

Nonlinear function expansion

$$y = f(\vec{x}) \cong g(\vec{x}) \equiv f^{NN}(\vec{x}) \Rightarrow \sum_{i=1}^{I} w_i \sigma(\vec{v}_i \cdot \vec{x}) + w_0$$

$\sigma(\vec{v}_i \cdot \vec{x})$ Variable basis function

$w_i \quad \vec{v}_i$ Weights

$$\vec{v}_i = (v_0^i, v_1^i, \ldots v_M^i)$$

$$\vec{x} = (1, x_1, \ldots x_M)$$

RMT(Residual Minimization Training) NNCM(Neural Network Collocation Method) vs. CTM(Conventional Training Method)

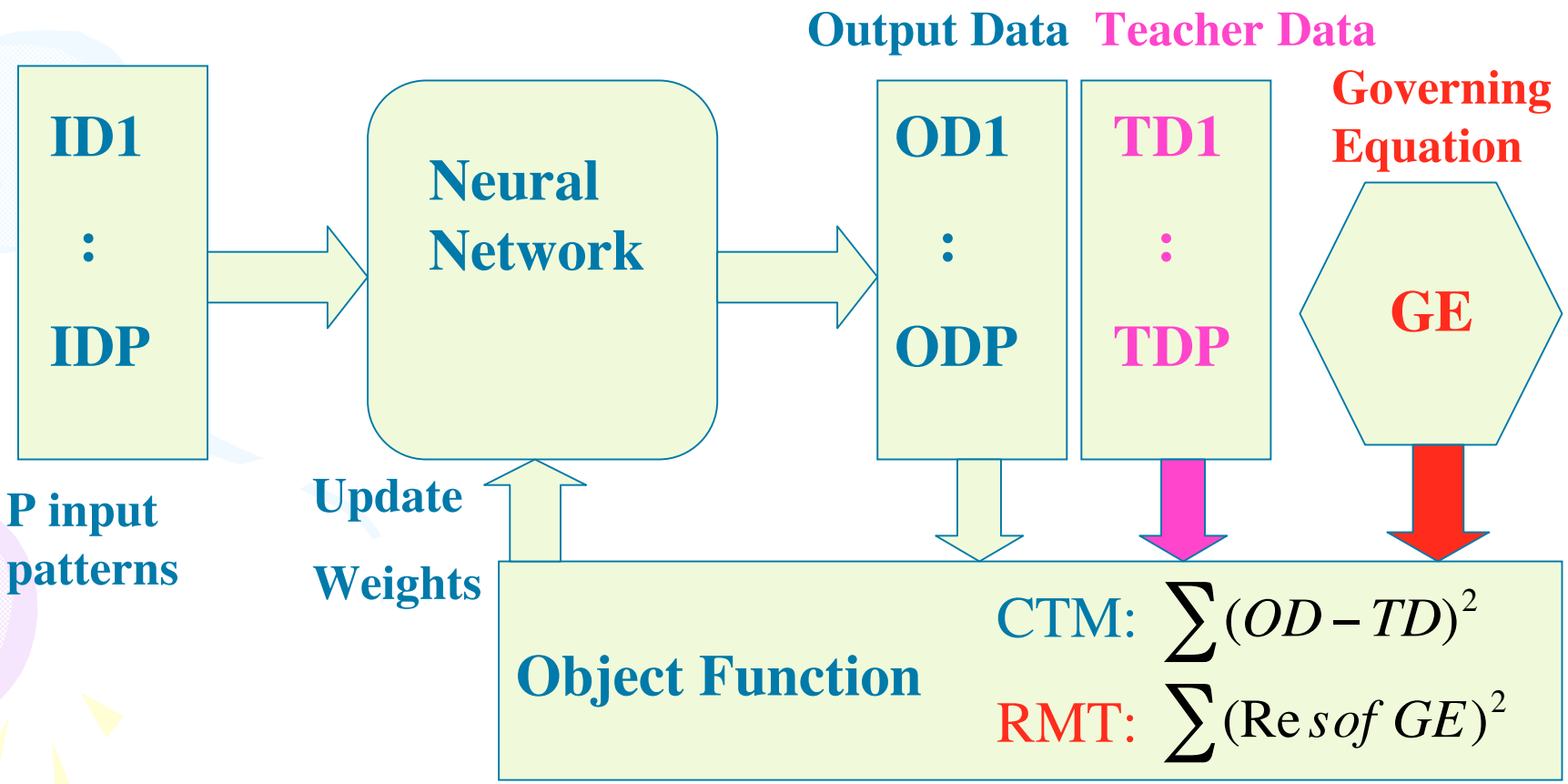

Training Data

(1) Conventional Training

P patterns of input dataset (ID1,…IDP) are prepared.

Teacher data corresponding to the input datasets are SUPPLIED(TD1,…TDP).

P sets of (ID-TD) are KNOWN EXAMPLES

(2) RMT/NNCM

P patterns of input dataset (ID1,…IDP) are COLLOCATION points in an input space.

Teacher data are NOT SUPPLIED.

P input patterns are COLLOCATION POINTS in the input space

2. Computerized tomography by neural network collocation method

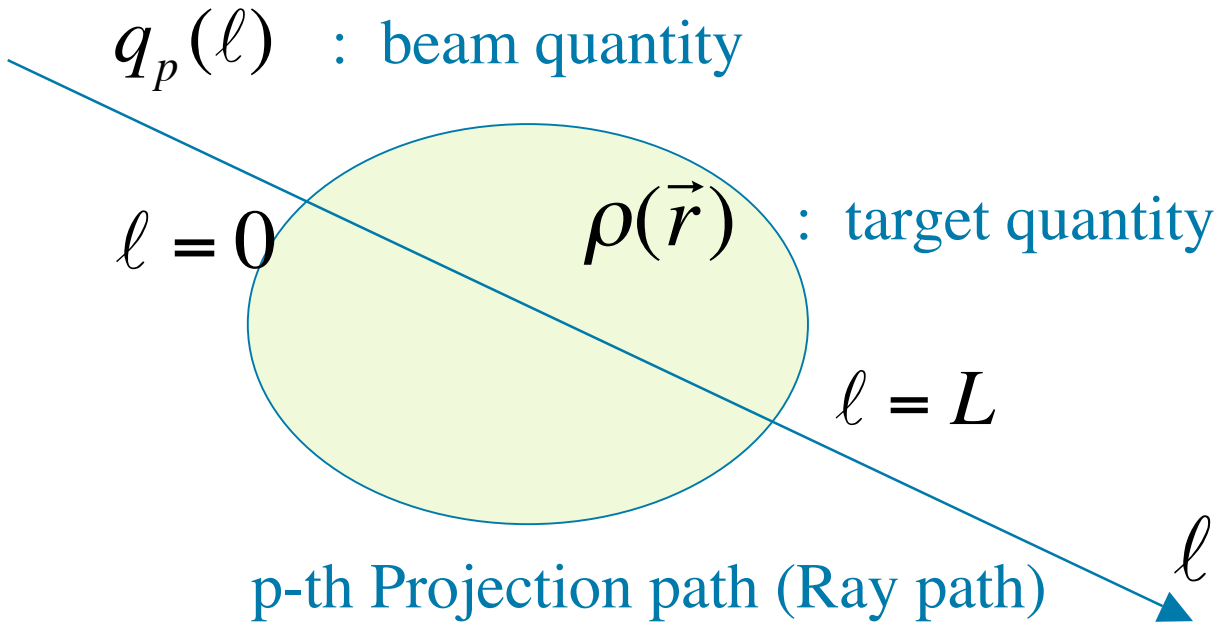

Our purpose is to reconstruct spatial distribution of the target quantity from measured change of the beam quantity for many projection paths.

Assumption: Variation of the beam quantity depends on the local value of the beam quantity and the target quantity

$$dq_p = f\left(\rho(\vec{r}), q_p\right) d\ell$$

In a phase delay type tomography such as CIT(Computerized Ionospheric Tomograph) the beam quantity (phase delay) does not depends on the beam quantity itself.

$$\Delta\phi_p \equiv \phi_p(L) - \phi_p(0) = A\int_{\ell=0}^{\ell=L,(p)} \rho(\vec{r})\, d\ell$$

In an attenuation type tomography the beam quantity is the beam intensity and the target quantity is the decay constant.

$$dN_p = -\mu(\vec{r}) N_p d\ell$$

$$N_p(L) = N_p(0)\exp\left[-\int_0^{L,(p)} \mu(\vec{r})\, d\ell\right]$$

Object function

$$E = \frac{1}{2}\sum_{p=1}^{P}\left(\Delta\phi_p^{NN} - \Delta\phi_p^{meas}\right)^2$$

$$\Delta\phi_p^{NN} = A\sum_{t=1}^{T,(p)}\alpha_t\rho(\vec{r}_t) \approx A\int_0^{L,(p)}\rho(\vec{r})d\ell$$

To update weight values EBP (Error Back-Propagation) is employed. EBP is essentially the gradient method.

$$\Delta w^{(\tau)} = -\eta A\left(\Delta\phi_p^{NN} - \Delta\phi_p^{meas}\right)\sum_{t=1}^{T}\alpha_t\left.\frac{\partial\rho(\vec{r}_t)}{\partial w}\right|_{w^{(\tau)}} + \beta\Delta w^{(\tau-1)}$$

Collocation points on a projection path p

$$\vec{X}_p = (\vec{x}_p^{(1)}, \ldots \vec{x}_p^{(T)}) \qquad \vec{Y}_p = (y_p^{(1)}, \ldots y_p^{(T)})$$

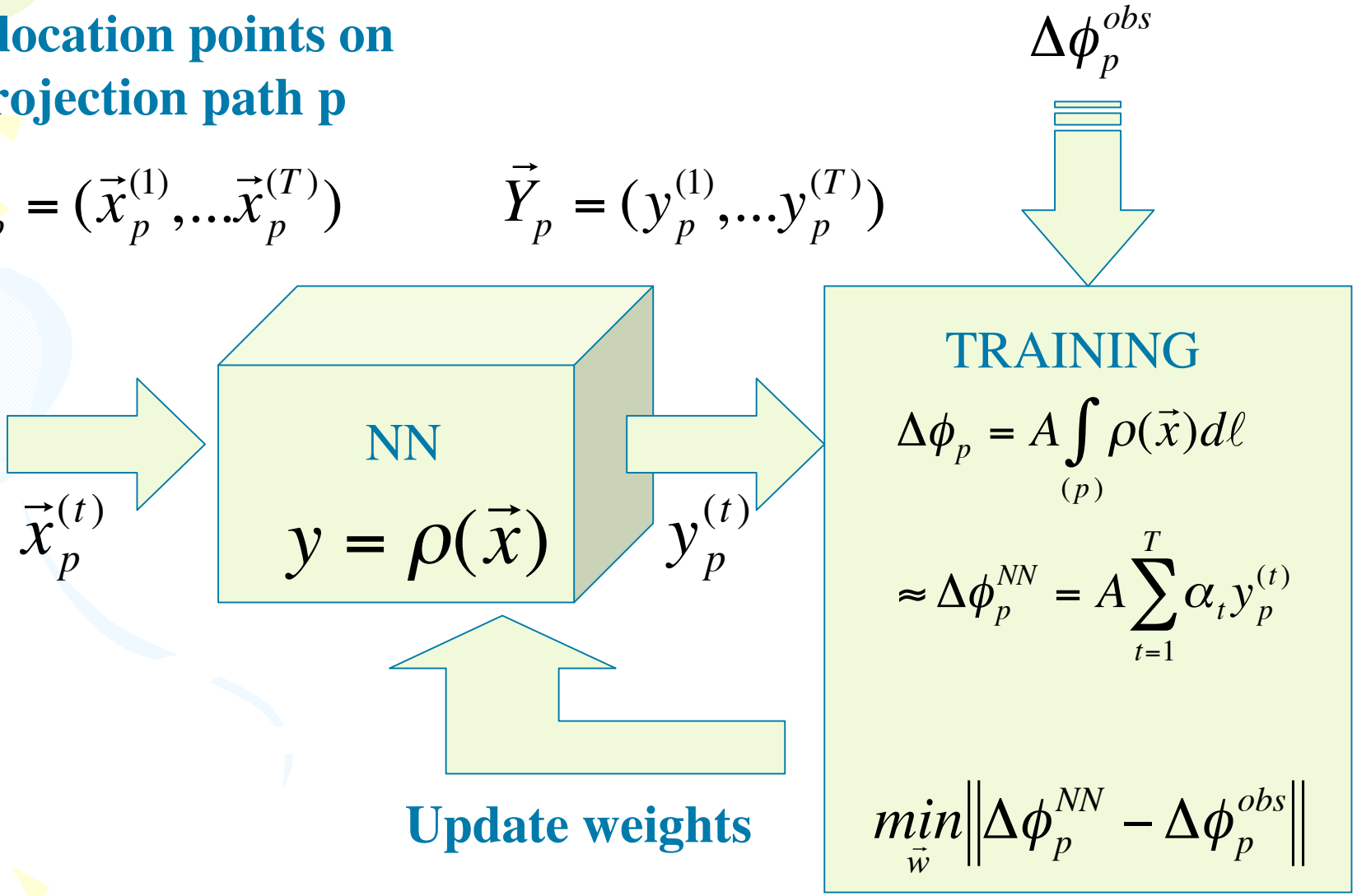

3. CT image reconstruction for small amount of model projection data

2D Computerized Tomography

Projection paths

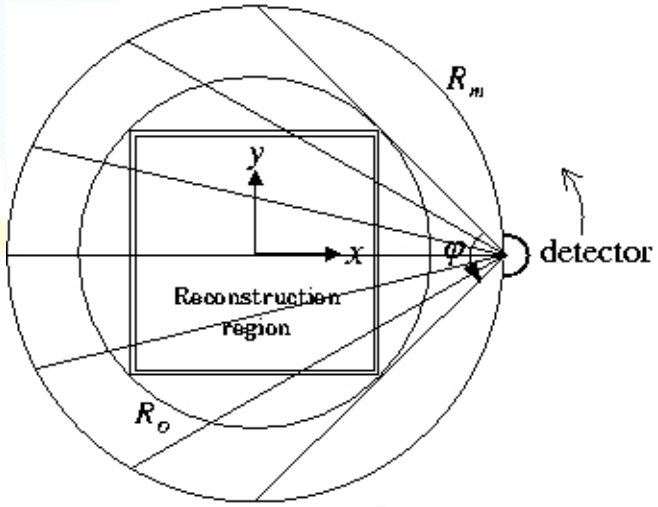

Fan-beam type paths

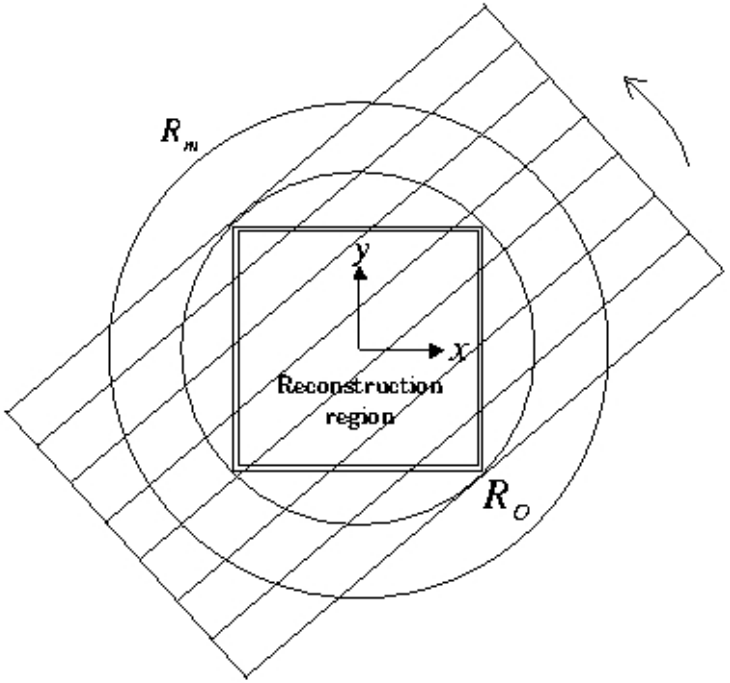

Parallel-beam type paths

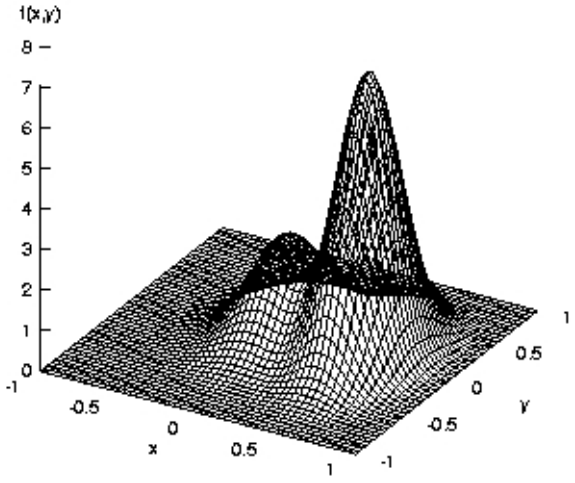

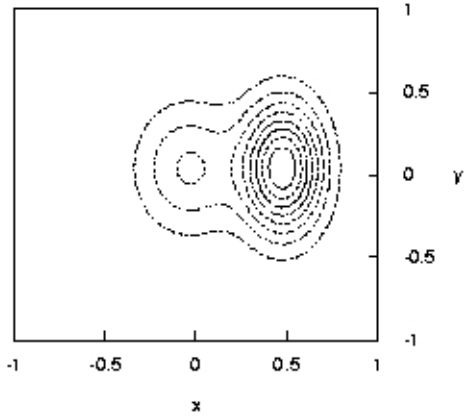

Model distribution

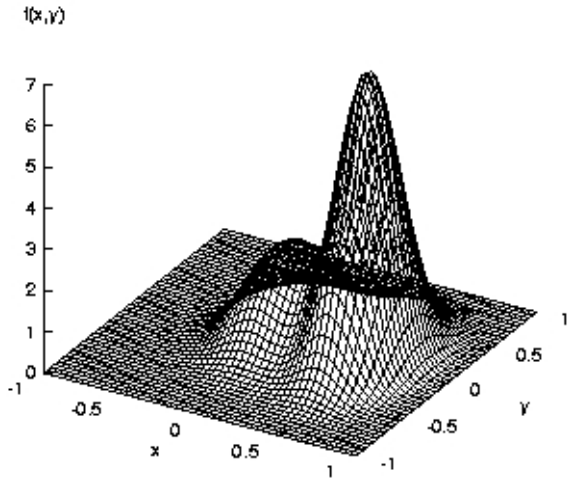

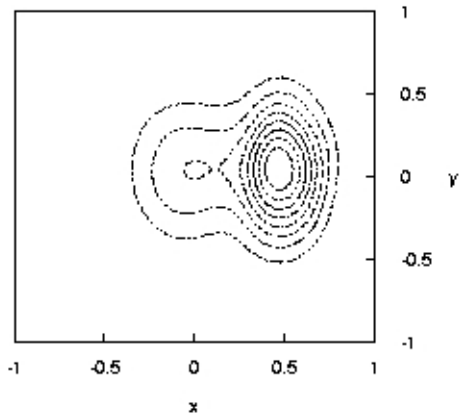

30x30=900

fan-beam

without noise

Ef=0.0191

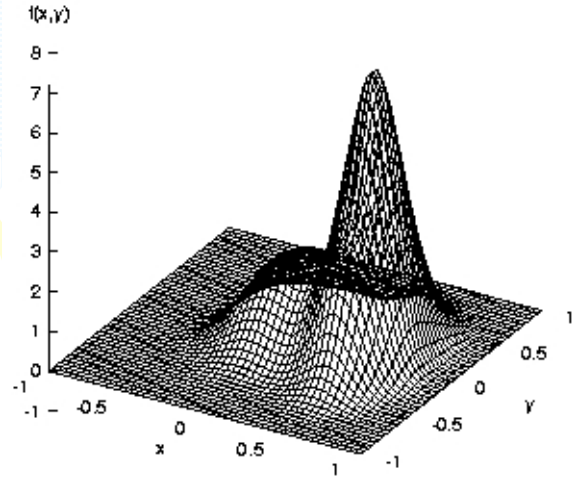

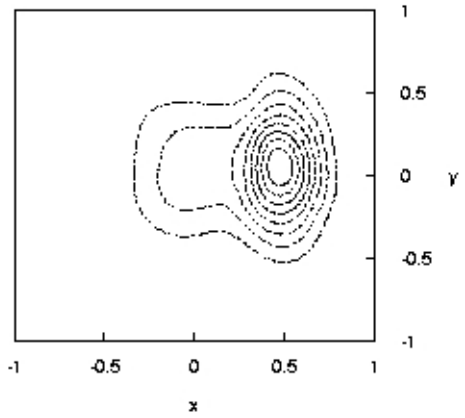

30x30=900

fan-beam

with noise

Ef=0.0267

$$E_f = \sqrt{\frac{\sum_N (z_{org} - z_{rec})^2}{N z_{\max}}}$$

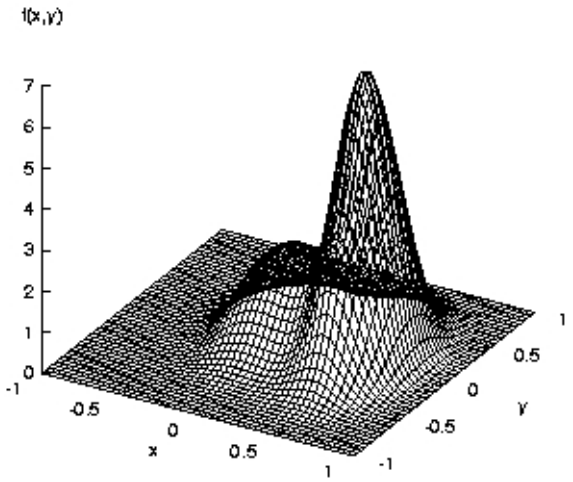

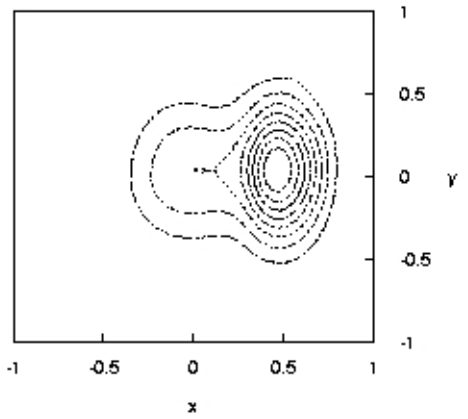

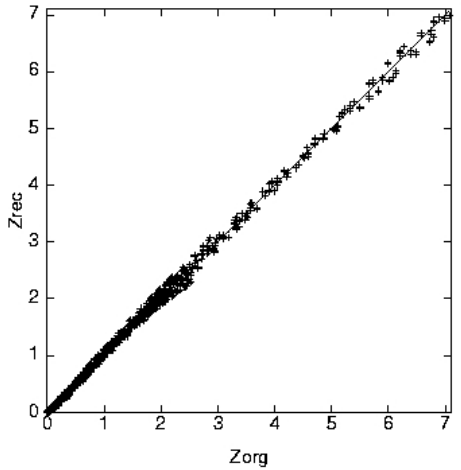

NNCM, 30x30=900, Parallel-beam, Ef=0.0219

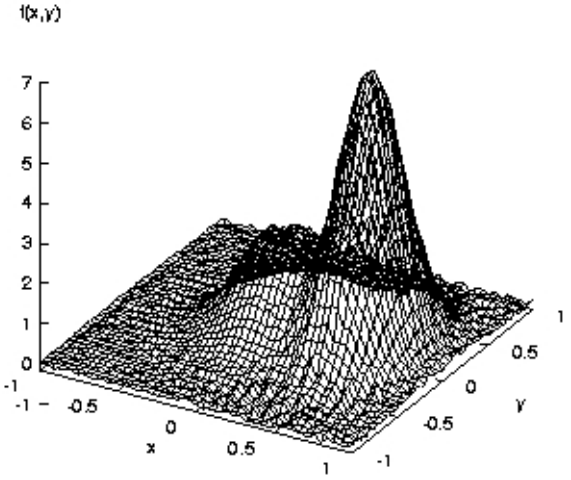

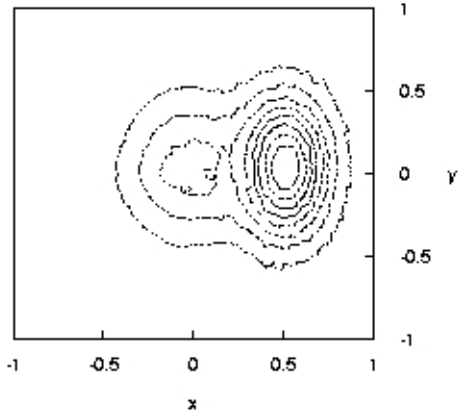

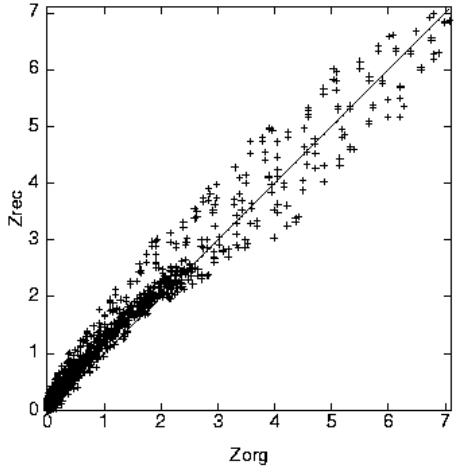

FBP, 30x30=900, Parallel-beam, Ef=0.143

Extremely small amount of projection paths

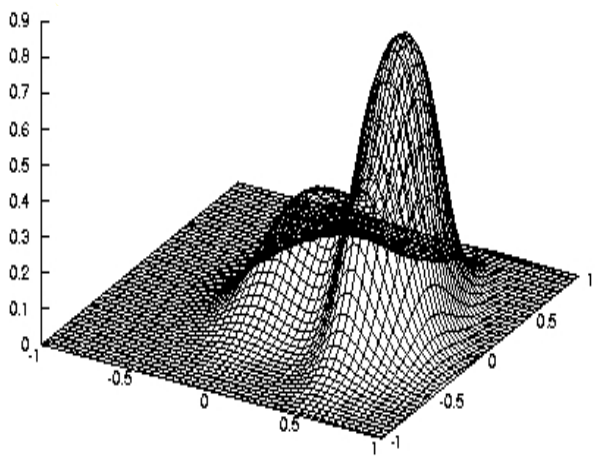

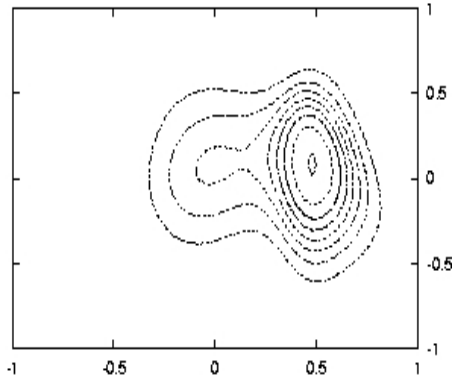

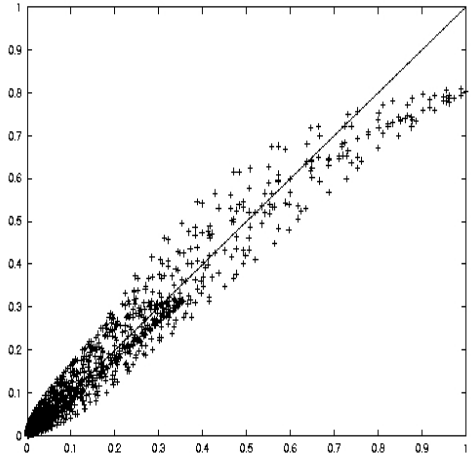

3x10=30, Fan-beam, Ef=0.034

4. CT image reconstruction of ionospheric electron density distribution by NNCM

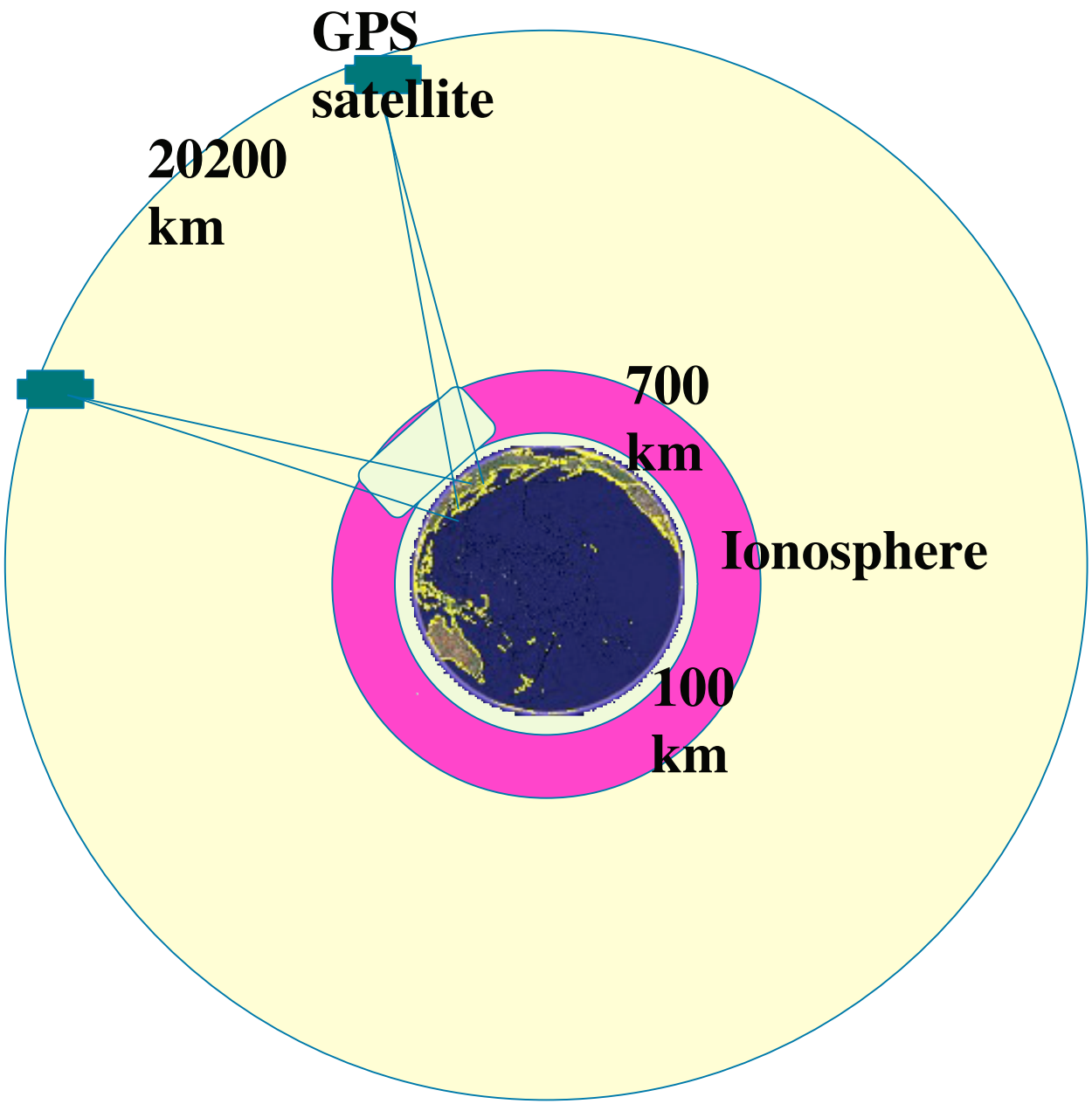

4.1 Some issues specific to the CT of the ionospheric electron distribution

Governing equations

$$I_i^j(t) = \int_{\vec{r}_i}^{\vec{r}_j} N(\vec{r},t)d\ell + B_i + B^j$$

$$(i = 1,...I; j = 1,...J)$$

$I_i^j(t)$ The slant TEC of the path from the transmitter of the satellite j to the ground receiver i

$N(\vec{r},t)$ The electron density

B_i The instrumental bias of the ground receiver i

B^j The instrumental bias of the transmitter j

Discretization

$$I_i^j(t) \approx \sum_{\ell=1}^{L} \alpha_\ell N(\vec{r}_\ell, t) + B_i + B^j + P_i^j$$

$$(i = 1,...I; j = 1,...J)$$

Penalized object function

$$E = gE_1 + E_2$$

The TEC term where P_i^j is the contribution from plasmaspheric electrons

$$E_1 = \sum_{i,j} \left(\sum_{\ell=1}^{L} \alpha_\ell N(\vec{r}_\ell, t) + B_i + B^j + P_i^j - I_i^j(t) \right)$$

The ionosonde term: the peak electron density at the corresponding height

$$E_2 = \sum_{s=1}^{S} \left(N_s(\vec{r}_s^{\,iono}) - N_s^{iono}(\vec{r}_s^{\,iono}) \right)^2$$

Contribution of electron distribution in the plasmasphere (700 ~ 20,200 km)

Model: a simple diffusive equilibrium model

$$n(h) = n(h_0)\exp\left(-\frac{h-h_0}{H_s}\right)$$

$$P_i^j = \frac{1}{\cos\theta}\int_{h_0}^{h_{sat}} n(h_0)\exp\left(-\frac{h-h_0}{H_s}\right)dh$$

$$= \frac{1}{\cos\theta} n(h_0)H_s\left(1-\exp\left(\frac{h_{sat}-h_0}{H_s}\right)\right)$$

$$\approx \frac{1}{\cos\theta} n(h_0)H_s$$

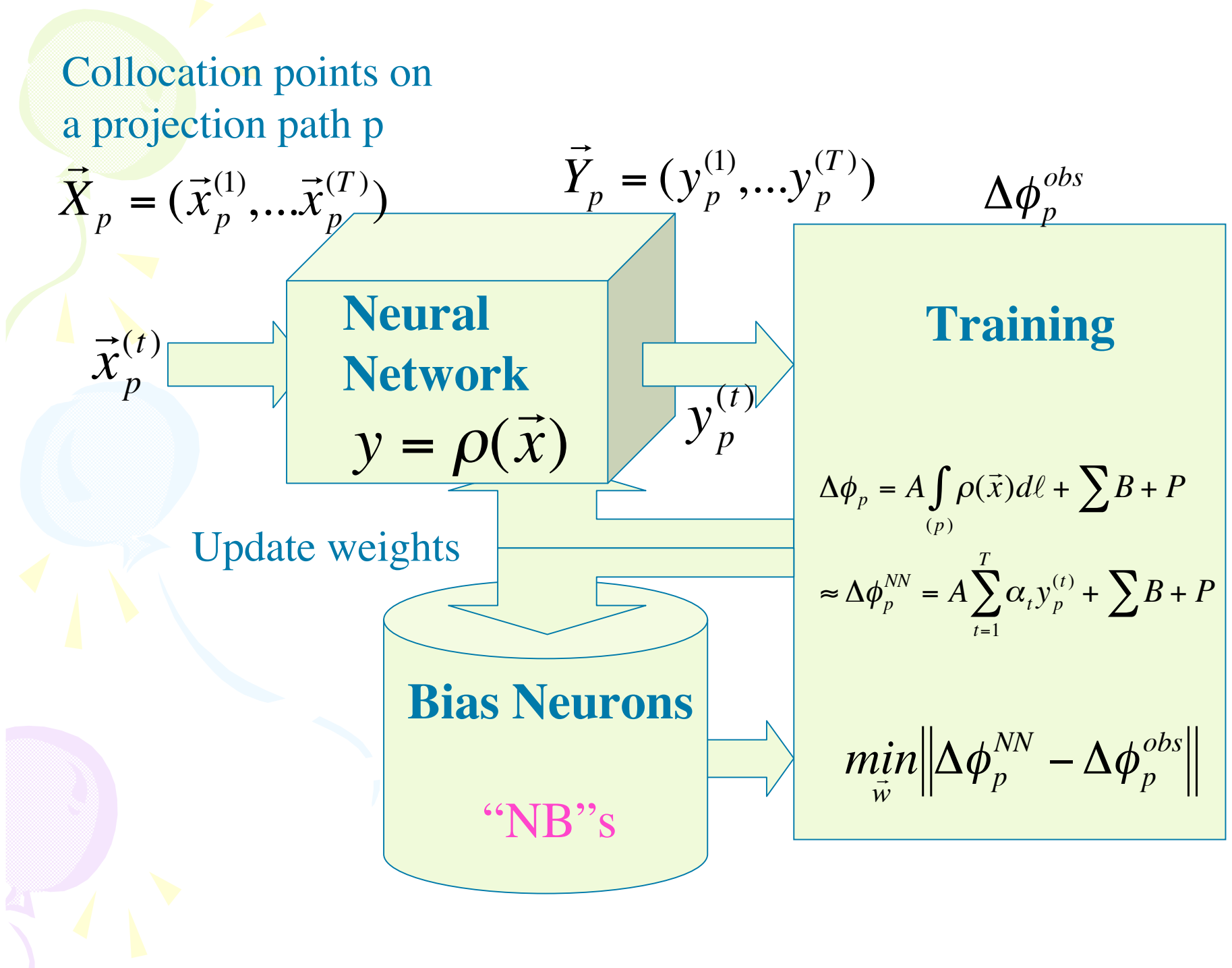
Collocation points on
a projection path p
$\vec{X}_p = (\vec{x}_p^{(1)}, \ldots \vec{x}_p^{(T)})$
$\vec{Y}_p = (y_p^{(1)}, \ldots y_p^{(T)})$
$\Delta\phi_p^{obs}$
$\vec{x}_p^{(t)}$
Neural
Network
$y = \rho(\vec{x})$
$y_p^{(t)}$
Training
$\Delta\phi_p = A\int_{(p)} \rho(\vec{x})d\ell + \sum B + P$
$\approx \Delta\phi_p^{NN} = A\sum_{t=1}^{T} \alpha_t y_p^{(t)} + \sum B + P$
Update weights
Bias Neurons
"NB"s
$\min_{\vec{w}} \left\| \Delta\phi_p^{NN} - \Delta\phi_p^{obs} \right\|$

4.2 Numerical experiment on model data

Model: the Global Core Plasma Model (GCPM)

which includes ionosphere

(International Reference Ionosphere: IRI)

plasmasphere,

magnetospheric trough

polar cap

Model data: the GCPM data of 1200-1215 JST December 2001 (0300-0315 UT December 2001)

Observation stations

(for both the model experiment and the real data analysis)

GPS receivers: the 40 GEONET receivers

Ionosonde for analysis: Kokubunji (35.74 N, 139.51 E)

Ionosonde for validation: Wakkanai (45.23 N, 141.41 E)

Yamagawa (31.12 N, 130.37 E)

Okinawa (26.16 N, 127.48 E)

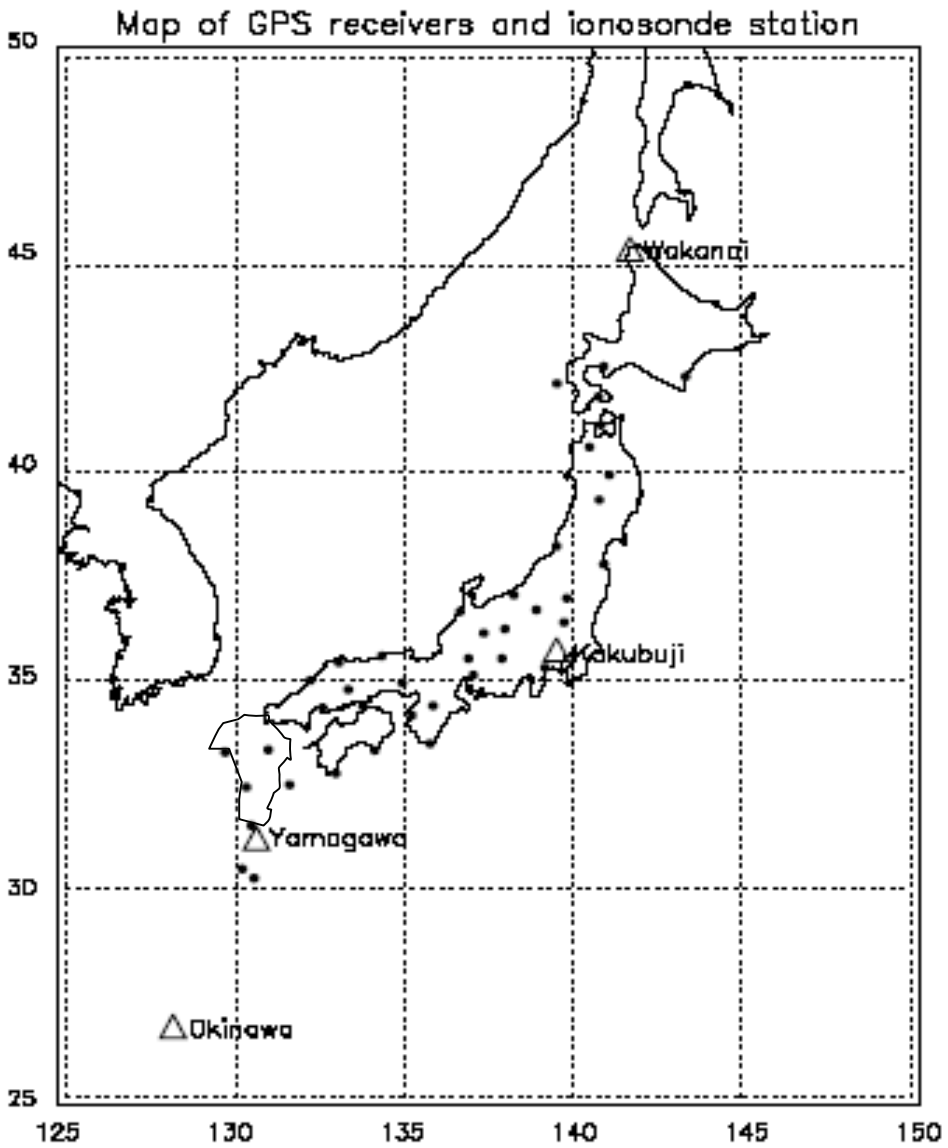
Map of GPS receivers and ionosonde station
50
45
40
35
30
25
125
130
135
140
145
150
Wakkanai
Kokubuji
Yamagawa
Okinawa

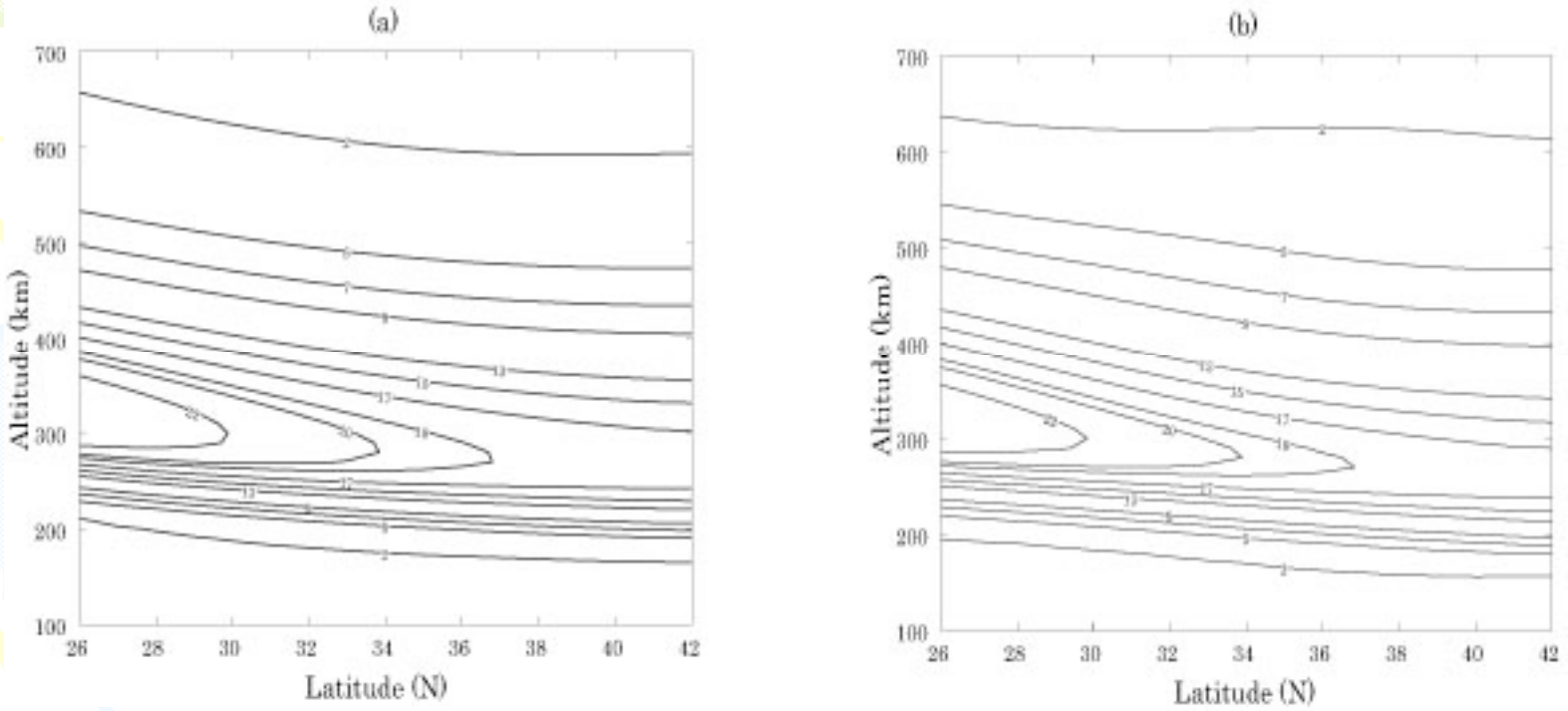

Contour plot of the model (a) and reconstructed (b) density distributions at longitude 137 E. The unit of density is 10^{11} m^{-3}.

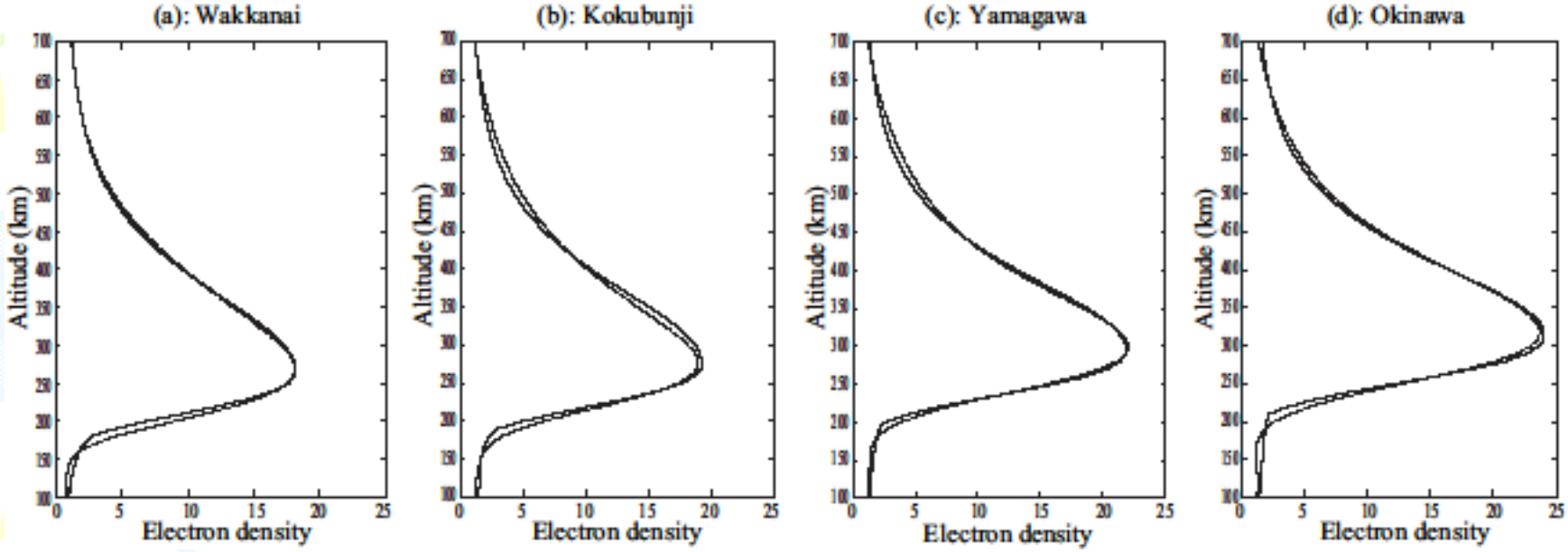
(a): Wakkanai
(b): Kokubunji
(c): Yamagawa
(d): Okinawa
Altitude (km)
Electron density

4.3 Reconstruction of real electron density distribution

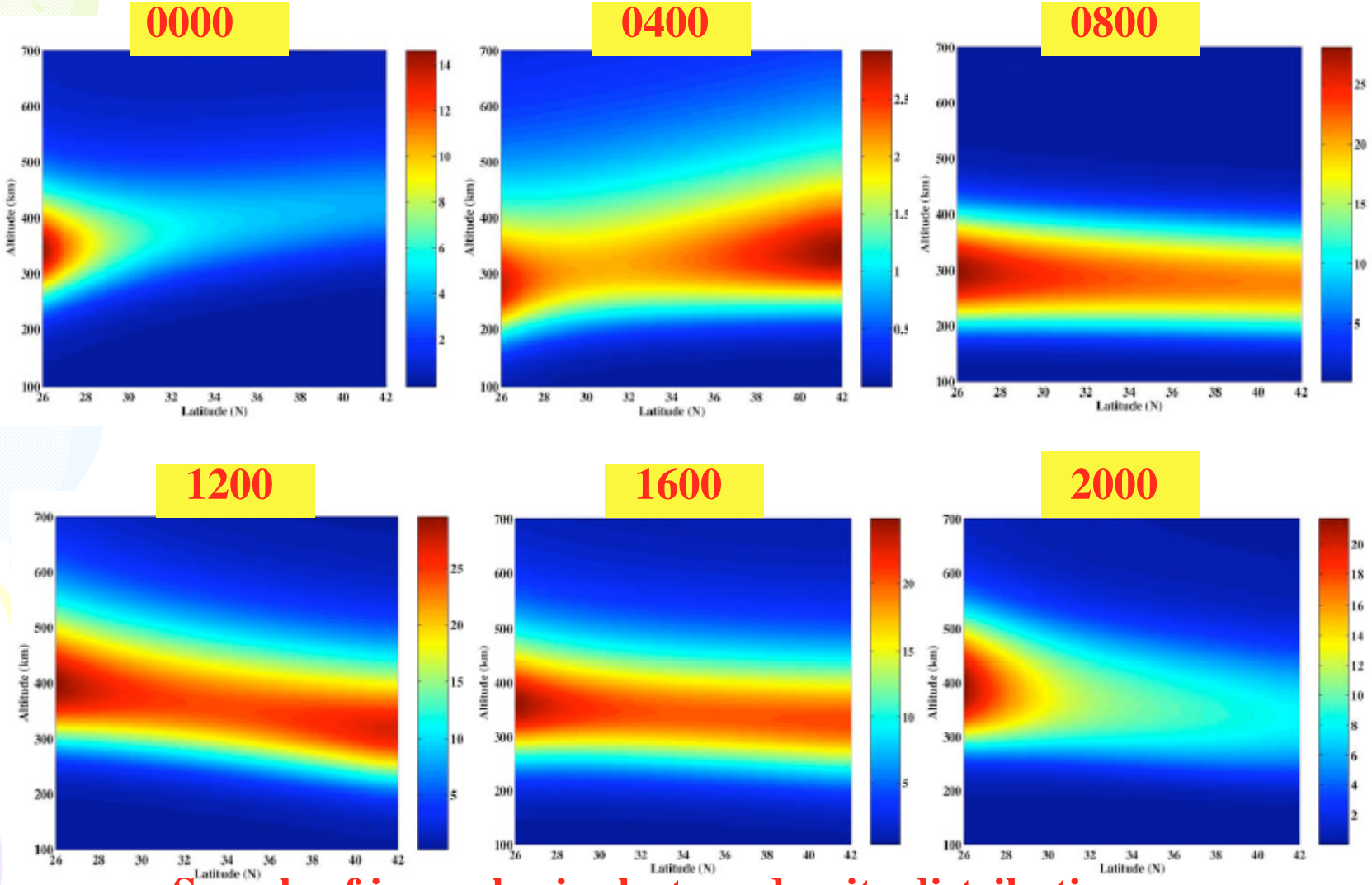

Sample of ionospheric electron density distribution

Nov.5, 2001(Longitude:137 E, Latitude:26 N~42 N)

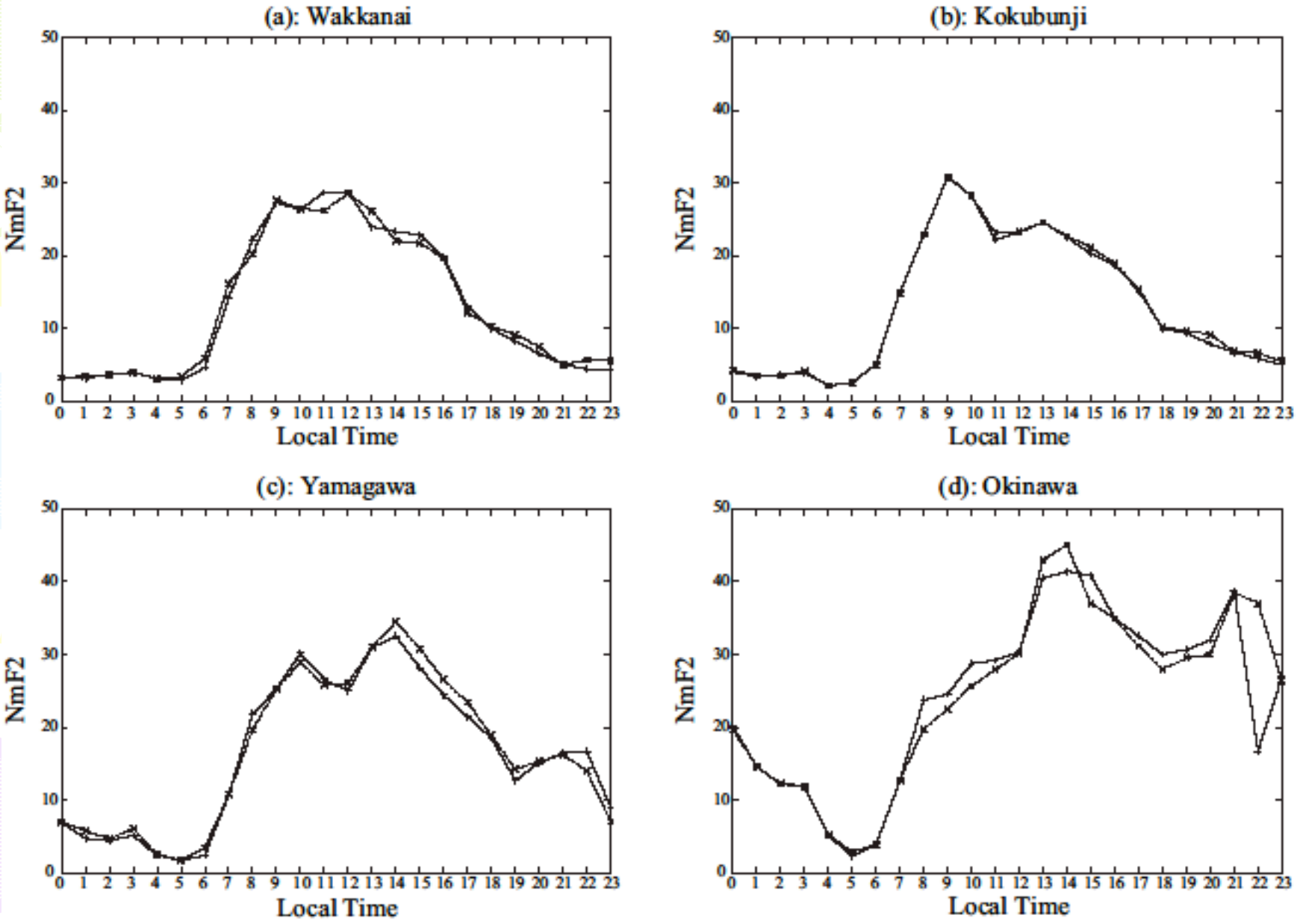

NmF2 vs Local Time for 4 ionosonde stations

NmF2 at 4 ionosonde stations

for local time t=0, 4, 8, 12, 16, 20

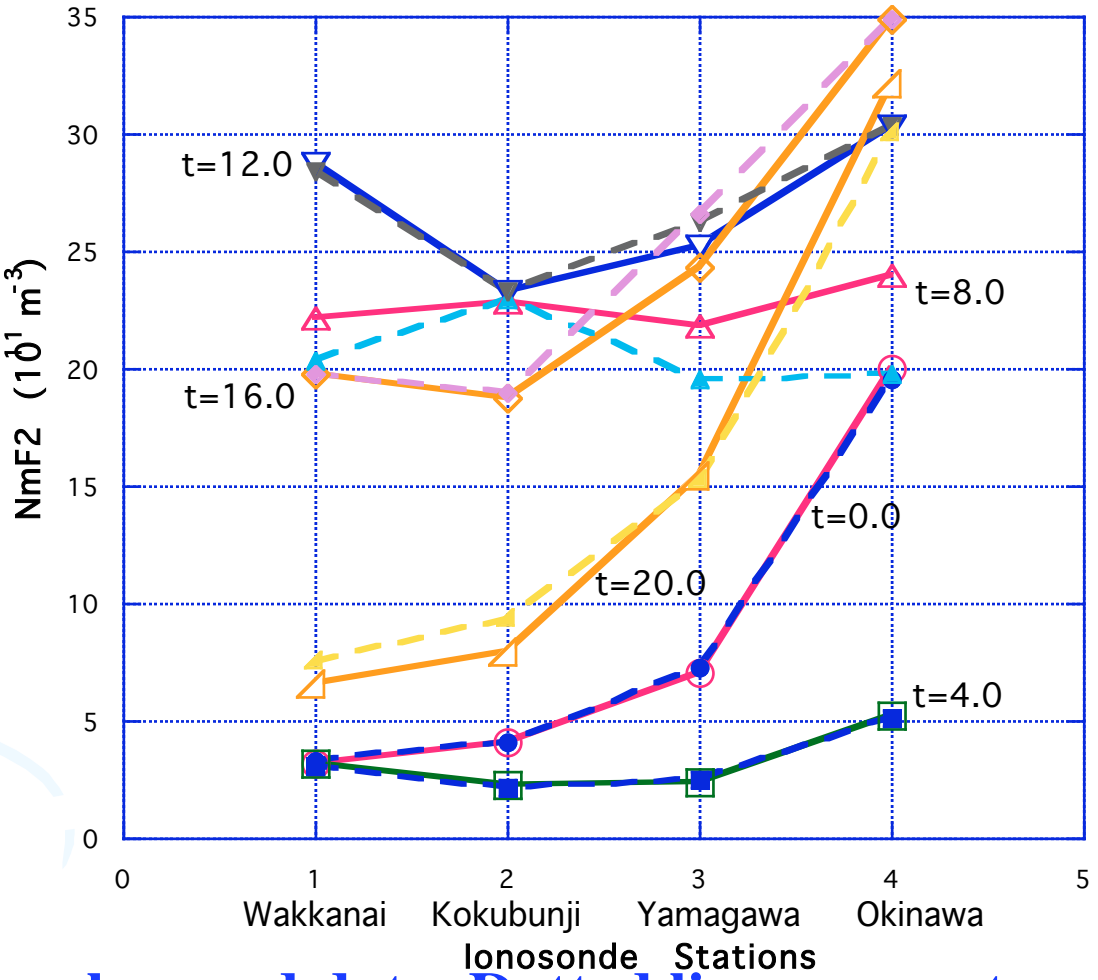

Solid line: observed data, Dotted line: reconstructed data

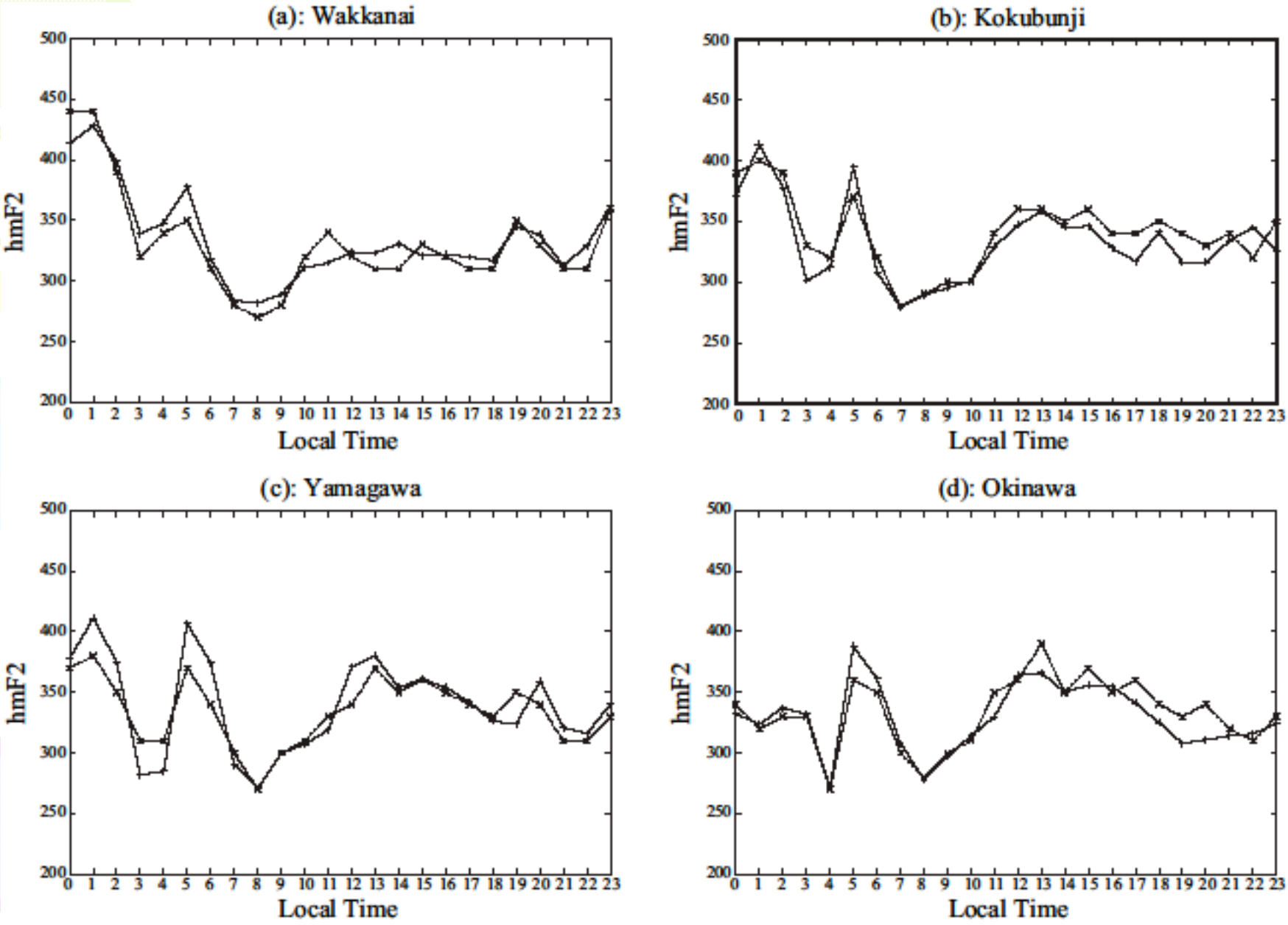

NmF2 vs Local Time for 4 ionosonde stations

hmF2 at 4 ionosonde stations

for local time t=0, 4, 8, 12, 16, 20

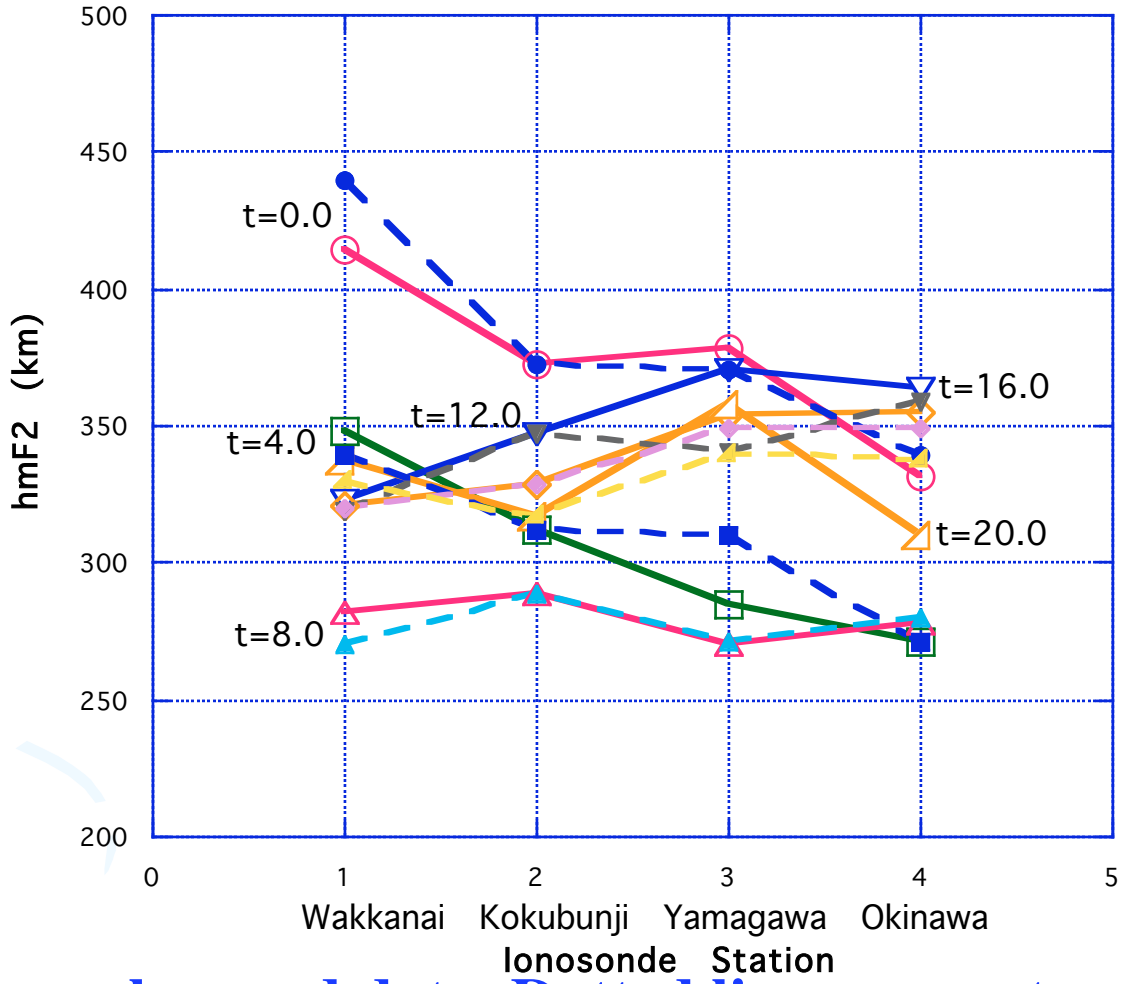

Solid line: observed data, Dotted line: reconstructed data

5. Conclusion

We have successfully applied NNCM based on NNRMT to to three-dimensional CIT

The following three ideas are effective for our purpose
- Skimmer-type activation function and
- Input space discretization for stable convergence
- Use of ionosonde data for vertical resolution

It is conjectured that the effectiveness of NNCM for the CIT may be attributed to the fact that a neural network is considered to be a function approximation by variable basis functions.

To numerically solve a problem of the CT image reconstruction it is necessary to use, explicitly or implicitly, a function expansion using SOME BASIS FUNCTIONS.

The most important feature of NNCM is that it uses VARIABLE BASIS FUNCTIONS.

In the next slide we summarize the basis functions used for different methods of CT image reconstruction.

Method	Basis Functions		Problems
ART	Fixed Orthogonal Function Series	1 in each pixel	Smoothness of solution
FBP Fourier Slice Theorem		Mathematical Basic or Special Functions	Nonuniformity Scarcity of projection data
Ad Hoc Methods (CIT etc)		EOF of model distribution	Model dependency
NNCM	Variable Basis Functions (NN etc)		

References

[1] T. Takeda, A. Liaqat, and M. Fukuhara, *Proc. Internat. Workshop on Modern Sc. and Technol. 2002* (Sept. 19-20, Univ. of Electro-Commun., Tokyo, 2002) p.145,

[2] X. F. Ma, M. Fukuhara, and T. Takeda, Nucl. Instrum. Methods in Phys. Res. **A 449**, 366 (2000).

[3] X. F. Ma, T. Maruyama, G. Ma, and T. Takeda, J. Geophys. Res. **110**, A05308, doi:10.1029/2004JA010797 (2005).

[4] J. R. Austen, S. J. Franke, and C. H. Liu, Radio Sci. **23**, 299 (1988).

[5] T. D. Raymund, J. R. Austen, S. J. Franke, C. H. Liu, J. A. Klobuchar, and J Stalker, Radio Sci. **25**, 771 (1990).

[6] F. J. Fremouw, J. A. Secan, and B. M. Howe, Radio Sci. **27**, 721 (1992).

[7] M. Kunitake, K. Ohtaka, T. Maruyama, M. Tokumaru, A. Morioka, and S.Watanabe, Ann. Geophysicae **13**, 1303 (1995).

[8] G.A. Hajj and L. J. Romans, Radio Sci. **33**, 175 (1998).

[9] L.-C.Tsai, W. H. Tsai, W. S. Schreiner, F. T. Berkey, and J. Y. Liu, Earth Planets Space **53**, 193 (2001).

[10] M. Garcia-Fernandez, M. Hernandez-Pajares, M. Juan, and J.Sanz, J. Geophys. Res. **108**(A9) 1338, doi:10.1029/2003JA009952 (2003).
[11] A. J. Hansen, T. Walker, and P. Enge, Ionospheric correction using tomography, *Proceedings of the Institute of Navigation GPS'97*, 249 (1997).
[12] M. J. Hernandez-Pajares, M. Juan, and J. Sanz, J. Geophys. Res. **103**, 20,789 (1998).
[13] S. Miyazaki, T. Saito, M. Sasaki, Y. Hatanaka, and Y. Iimura, Bull. Geogr. Surv. Inst. **43**, 23 (1997).
[14] S. Haykin, *Neural Networks: A Comprehensive foundation*, 2nd Ed. (Prentice Hall, Upper Saddle River, NJ, 1999)
[15] R. Rojas, *Neural Networks: A Systematic Introduction* (Springer, Berlin, 1996).
[16] D. E. Rumelhart, G. E. Hinton, and R. J. Williams, Nature **323**, 533(1986).
[17] K. Funahashi, Neural Networks **2**, 183 (1989).
[18] H. White, Neural Networks **3**, 535 (1990).
[19] T. Poggio, and G. Girosi, Science **247**, 978 (1990).

[20] J. J. Angerami and J. O. Thomas, J. Geophys. Res. **69**, 4537 (1964).
[21] D. L. Gallagher and P. D. Craven, J. Geophys. Res. **105**, 18,189 (2000).
[22] D. Blitza, *International Reference Ionosphere 1990, NSSDC 90-22*, Natl. Space Sci. Data Center, Greenbelt, Md (1990).
[23] X.F. Ma and T. Takeda, Nucl. Instr. Methods in Phys. Res. **A 492**, 178 (2002).
[24] A. Liaqat, M. Fukuhara, and T. Takeda, Comput. Phys. Commun. **141**, 350 (2001).
[25] A. Liaqat, M. Fukuhara, and T. Takeda, Comput. Phys. Commun. **150**, 215 (2003).
[26] A. Liaqat, M. Fukuhara, and T. Takeda, Month. Weather Rev. **131**(8) 1696 (2003).
[27] J. Wu, M. Fukuhara, and T. Takeda, Ecological Modeling **189**, 289 (2005).
[28] X.F. Ma, T. Maruyama, G. Ma, and T. Takeda, Radio Sci. **40**, RS1002, doi:10.1029/2004RS003072 (2005).